Tunable generic model for fluid bilayer membranes

Ira R. Cooke, Kurt Kremer, and Markus Deserno
Max-Planck-Institut für Polymerforschung, Ackermannweg 10, 55128 Mainz, Germany
(Received 23 September 2004; revised manuscript received 9 June 2005; published 26 July 2005)

We present a model for the efficient simulation of generic bilayer membranes. Individual lipids are represented by one head bead and two tail beads. By means of simple pair potentials these robustly self-assemble to a fluid bilayer state over a wide range of parameters, *without* the need for an explicit solvent. The model shows the expected elastic behavior on large length scales, and its physical properties (e.g., fluidity or bending stiffness) can be widely tuned via a single parameter. In particular, bending rigidities in the experimentally relevant range are obtained, at least within $3-30k_BT$. The model is naturally suited to study many physical topics, including self-assembly, fusion, bilayer melting, lipid mixtures, rafts, and protein-bilayer interactions.

DOI: 10.1103/PhysRevE.72.011506 PACS number(s): 61.20.Ja, 81.16.Dn, 82.70.Uv

Lipid molecules in aqueous solution spontaneously assemble into bilayer membranes. In biological systems, such membranes are involved in tasks over an extraordinary range of length scales, from transport of water and ions at the scale of nanometers, up to phagocytosis, amoebal motion and cell budding at the scale of microns [1]. Computer simulations designed to understand some aspects of this structural and functional range must be tailored to the specific length and timescales involved. Techniques that probe both the smallest [2] and largest [3] of these length and time scales are now well established; however, accessing intermediate regimes has proven far more difficult, and it is only recently that significant progress has been made in this regard. The need for a comprehensive suite of techniques to study lipid bilayers at the mesoscale is highlighted by the sheer number of relevant problems in this regime, which include viral budding, raft formation, fusion, phase separation of multicomponent systems, and protein sorting during vesiculation.

Most existing approaches to mesoscale simulation employ coarse grained lipids and require explicit solvent particles to stabilize the bilayer. This strategy is convenient and natural, yet it comes at a high price: Already for small flat systems the solvent accounts for most of the computational effort, but the problem gets significantly worse when three dimensional objects such as vesicles are to be simulated. Membrane and solvent play the role of surface and bulk, respectively, hence, the solvent degrees of freedom vastly outnumber the lipids even for rather modest sized vesicles. An obvious solution to this problem is to replace the solvent by effective lipid interactions. Given the great success of this approach in polymer physics it is perhaps surprising that solvent-free bilayer simulations have so far failed to find widespread acceptance. The problem appears to be that naive choices for interparticle potentials (e.g., Lennard-Jones) do not lead to a fluid bilayer phase but only to ordered "solid" bilayers at low temperature and low density phases at high temperature. Many attempts to obtain a broadly stable fluid phase have been made with varying degrees of success. So far, however, none of these has resulted in a model that is sufficiently robust, simple, or versatile for general use. For example, the original solvent-free model of Drouffe *et al.* [4] and later modifications by Noguchi [5] rely on density dependent interaction potentials to stabilize the fluid phase. But the multibody nature of interactions poses serious problems for interpretation and measurement of thermodynamic quantities. Other models do not exhibit the crucial property of unassisted self-assembly [6,7] and require the use of angular dependent potentials [7] or a large set of highly tuned interaction parameters [6]. Thus, there remains a clear need for an efficient, robust, and tunable solvent-free bilayer model.

Let us now describe such a model. Its key ingredient is an attraction between lipid tails the *range* of which can be varied. Each lipid molecule is represented by one "head" bead followed by two "tail" beads. Their size is fixed via a Weeks-Chandler-Andersen potential

$$V_{\mathrm{rep}}(r;b)=\begin{cases}4\epsilon\left[\left(\frac{b}{r}\right)^{12}-\left(\frac{b}{r}\right)^{6}+\frac{1}{4}\right], & r\leqslant r_c\\ 0, & r>r_c,\end{cases} \tag{1}$$

with $r_c=2^{1/6}b$. We use ϵ as our unit of energy. To ensure an effective cylindrical lipid shape we choose $b_{\mathrm{head,head}}=b_{\mathrm{head,tail}}=0.95\sigma$ and $b_{\mathrm{tail,tail}}=\sigma$, where σ is the unit of length. The three beads are linked by two FENE bonds

$$V_{\mathrm{bond}}(r)=-\frac{1}{2}k_{\mathrm{bond}}r_\infty^2\log[1-(r/r_\infty)^2], \tag{2}$$

with stiffness $k_{\mathrm{bond}}=30\epsilon/\sigma^2$ and divergence length $r_\infty=1.5\sigma$. Lipids are straightened by a harmonic spring with rest length 4σ between head bead and second tail bead

$$V_{\mathrm{bend}}(r)=\frac{1}{2}k_{\mathrm{bend}}(r-4\sigma)^2, \tag{3}$$

which corresponds in lowest order to a harmonic bending potential $\frac{1}{2}k_{\mathrm{bend}}\sigma^2\vartheta^2$ for the angle π-ϑ between the three beads. We fixed the bending stiffness at $k_{\mathrm{bend}}\sigma^2=10\epsilon$. Finally, all *tail* beads attract according to

$$V_{\mathrm{attr}}(r) = \begin{cases} -\epsilon, & r < r_c \\ -\epsilon \cos^2 \dfrac{\pi(r - r_c)}{2w_c}, & r_c \leqslant r \leqslant r_c + w_c \\ 0, & r > r_c + w_c. \end{cases} \quad (4)$$

This describes an attractive potential with a depth of ϵ which for $r > r_c$ smoothly tapers to zero. Its decay range w_c is the key tuning parameter in our model.

We performed molecular dynamics (MD) simulations using the ESPResSo package [8]. A fixed number of lipids was simulated in a cubic box of side length L subject to periodic boundary conditions. The canonical state was reached by means of a Langevin thermostat [9] (with a time step $\delta t = 0.01\tau$ and a friction constant $\Gamma = \tau^{-1}$ in Lennard-Jones units). If needed, constant tension conditions were also implemented via a modified Andersen barostat [10] (with a box friction $\Gamma_{\mathrm{box}} = 2 \times 10^{-4}\tau^{-1}$ and box mass within the range $Q = 10^{-5} \cdots 10^{-4}$).

One of our key objectives is to map out the conditions under which the fluid bilayer is stable. We identified the fluid phase in two different ways. First, a box-spanning bilayer was pre-assembled from 1000 lipids, and its equilibration under zero lateral tension was attempted (requiring—if successful—box lengths of $L \approx 25\sigma$). Three qualitatively different outcomes were observed: (i) At sufficiently low temperature the bilayer adopted a "gel" phase; (ii) within a more elevated temperature range a fluid phase can be reached, *provided* $w_c \gtrsim 0.8\sigma$; and (iii) at sufficiently high temperature a bilayer under zero tension always fell apart. Fluid and gel phases are clearly distinct under visual inspection (long range order in the gel phase and none in the fluid). Across the gel-fluid boundary [11] we observed a sharp increase of in-plane diffusion constant D, an abrupt decrease in orientational order $S = \frac{1}{2}\langle 3(\boldsymbol{a}_i \cdot \boldsymbol{n})^2 - 1 \rangle_i$ (where $\boldsymbol{a}_i$ is the vector along the axis of the ith lipid and $\boldsymbol{n}$ is the average bilayer normal) and the emergence of a nonzero flip-flop rate r_f (the probability per unit time that a single lipid changes its monolayer). Typical values along the $k_B T = 1.1\epsilon$ isotherm are $D = 0.06 - 0.03\sigma^2/\tau$, $S = 0.5 - 0.8$, and $r_f = 2 - 90 \times 10^{-5}\tau^{-1}$. For $w_c = 1.6\sigma$ and $k_B T = 1.1\epsilon$ we also measured the rupture tension $\Sigma_r \approx 2.5$ mN/m and the compressibility modulus at zero tension, $\mathcal{K} \approx 30$ mN/m (mapping to real length scales by assuming a bilayer thickness of 5 nm). While the rupture tension is close to the typical range for phospholipid bilayers ($\Sigma = 3 - 4$ mN/m [12]), the compressibility modulus is at the lower end $\mathcal{K} = 50 - 1700$ mN/m, depending on cholesterol content [13]). Second, lipids were simulated at constant volume, but starting from a random "gas" configuration. Under all conditions which previously gave stable tensionless membranes, a bilayer patch quickly self-assembled which at the right L could zip up with its open ends to span the box. If the box was too big, the patch either remained free, or (sometimes) closed upon itself to form a vesicle. Inside the fluid region of Fig. 1 these self-assembled bilayers exhibit a distinct bilayer structure with relatively little interdigitation between lipids. Box spanning bilayers could also occur somewhat above the evaporation boundary of Fig. 1 [14], indicating that this line should be viewed as the location

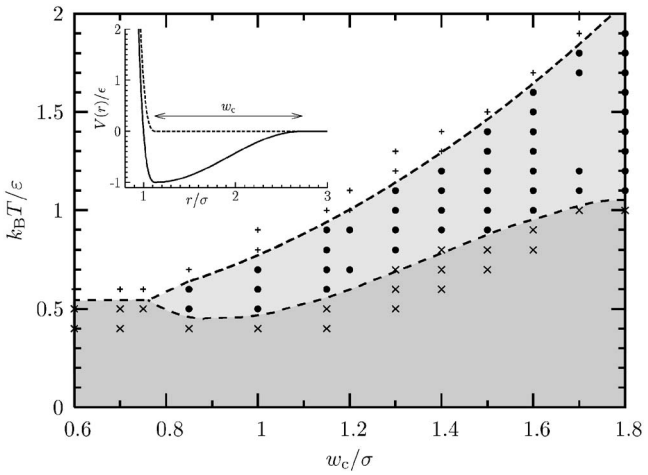

FIG. 1. Phase diagram in the plane of potential width w_c and temperature at zero lateral tension. Each symbol corresponds to one simulation and identifies different bilayer phases: ×: gel; ●: fluid, +: unstable. The dashed lines are merely guides to the eye. The inset shows the pair potential between tail lipids (solid line) and the purely repulsive head-head and head-tail interaction (dashed line).

where the rupture tension for a bilayer approaches zero. We finally remark that upon approaching this line from below, the bilayer becomes increasingly disordered, and flip-flop rates and diffusion constants increase strongly.

In Fig. 1 we see that the temperature range over which a fluid bilayer is stable increases as w_c is increased and that for relatively narrow potentials $w_c < 0.7\sigma$ the fluid region disappears completely [15]. It is noteworthy that these general features are not restricted to the present functional form of Eq. (4). Indeed, we have also obtained a qualitatively similar phase diagram for a Lennard-Jones (LJ) like potential with variable width. It should therefore be emphasized that it is not the precise functional form of our tail attractions that is important for the stabilization of fluid bilayers but rather the length scale over which these attractions are effective.

Next we illustrate that the fluid bilayers approach the correct elastic continuum limit. If one expands the bilayer in modes $h(\boldsymbol{r}) = \Sigma_{\boldsymbol{q}} h_{\boldsymbol{q}} e^{i\boldsymbol{q}\cdot\boldsymbol{r}}$ with $\boldsymbol{q} = 2\pi/L(n_x, n_y)$, (linearized) Helfrich theory predicts the spectrum [16]

$$\langle |h_{\boldsymbol{q}}^2| \rangle = \frac{k_B T}{L^2[\kappa q^4 + \sigma q^2]}, \quad (5)$$

where κ is the bending modulus and σ the lateral tension. Below the crossover wave vector $q_c = \sqrt{\sigma/\kappa}$ one has $\langle |h_{\boldsymbol{q}}^2| \rangle \sim q^{-2}$ (tension regime), while $\langle |h_{\boldsymbol{q}}^2| \rangle \sim q^{-4}$ holds above (bending regime). Once $1/q$ approaches length scales comparable to the bilayer thickness, continuum theory breaks down and further effects (e.g., protrusion modes [17]) set in. In order to see the characteristic q^{-4} scaling of the bending regime over a sufficiently wide range requires q_c to be as small as possible, hence we simulated at zero tension. Furthermore, to get away from microscopic lengths (such as the bilayer thickness) we took systems four times as big as the ones we used for mapping the phase diagram (4000 lipids, $L \simeq 50\sigma$). Note that reaching the continuum limit in MD

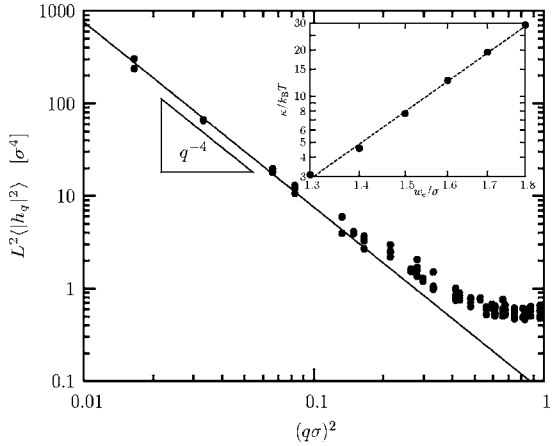

FIG. 2. Asymptotic q^{-4} scaling of the power spectrum $\langle|h_q^2|\rangle$ for the bilayer system with $w_c=1.6\sigma$ and $k_BT=1.1\epsilon$. The inset shows the thus measured bending stiffness values at fixed temperature ($k_BT=1.1\epsilon$) as a function of potential range w_c.

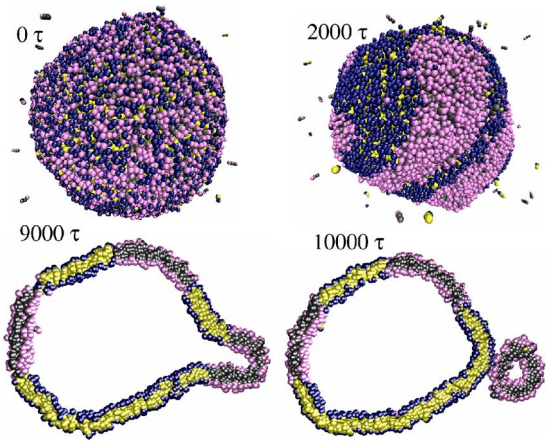

FIG. 3. (Color online) Phase separation and budding sequence for a mixed vesicle pre-assembled from 8000 *A* lipids and 8000 *B* lipids at $k_BT=1.1\epsilon$. After an equilibration time of 2000τ, during which $w_c^{AA}=w_c^{BB}=w_c^{AB}=1.5\sigma$, the cross term was reduced to $w_c^{AB}=1.3\sigma$. Times are measured from this point on.

simulations is not trivial, since the relaxation time of bending modes scales as q^{-4}.

After setting up the bilayer, we first waited until tension, box length, and energy had equilibrated (which took typically $10^5\tau$ for fluid systems). Then on the order of 100 configurations separated by 2000τ were used to measure the mode spectrum. The bilayer midplane was identified by tracking the tail beads and interpolating their vertical position onto a 16×16 grid. Stray lipids had to be excluded from this procedure. A fast Fourier transform (FFT) then yields the power spectrum $\langle|h_q^2|\rangle$. Figure 2 illustrates (for $w_c=1.6\sigma$ and $k_BT=1.1\epsilon$) the q^{-4} scaling. Notice that length scales exceeding $L\approx20\sigma$ (i.e., about four times the bilayer thickness) are required to reach the asymptotic regime, outside of which a fit to Eq. (5) and the subsequent extraction of a bending constant is meaningless. The inset shows the corresponding values of κ for the six simulated stable bilayer systems at this particular value of the temperature (see Fig. 1). We emphasize that its value is easily tuneable over the experimentally interesting range, at least from $\kappa\approx3k_BT$ up to $\kappa\approx30k_BT$.

So far we have used the parameter w_c only to tune the bilayer stiffness. Let us now illustrate another application, namely, the possibility of creating mixed lipid systems. We consider a simple example in which two lipid types *A* and *B* are present and where $w_c^{AA}=w_c^{BB}$. A line tension can now be generated by choosing the cross interaction w_c^{AB} smaller than the homogeneous ones. Provided a sufficiently small cross term has been chosen, *A* and *B* domains will form. Figure 3 illustrates qualitative features of this process for a critical quench ($A:B=1:1$). First we note that matching domains always appear on inner and outer leaflets. As is typical for a critical system, domains are initially elongated in shape and then coarsen to form circular patches or stripes. In this case the domain size and *A*-*B* line tension are sufficient to induce budding [18]. This process has recently been studied in detail via dissipative particle dynamics (DPD) simulations [19]. For matching lipid proportions in outer and inner leaflets, budding was induced by cleavage of the domain boundary. We also observed this "flaking mechanism" for very high line tensions ($w_c^{AB}\ll w_c^{AA,BB}$), while for less pronounced line tensions a more continuous type budding occured (see Fig. 3), provided the vesicle was big enough.

Next we investigate the kinetics of domain formation on a larger vesicle in the off-critical regime. Although this has been extensively studied for supported membranes, only a small number of recent simulations [19–21] and experiments [22] have tackled the problem for free vesicles. The importance of these studies is underscored by the fact that many features of a vesicular system are absent in a flat supported membrane. These include bending fluctuations, volume constraints, and kinetic effects of curvature-composition coupling [23].

To study the kinetics of phase separation we performed simulations using pre-equilibrated vesicles with an $A:B$ ratio of 3:7 and measured the number $n(t)$ of clusters of *A* lipids as a function of time. This quantity displays two distinct kinetic regimes (see Fig. 4). In the first regime $n(t)$ decays exponentially, corresponding to a conversion of an initially exponential cluster size distribution to an arrangement where mesosized clusters begin to dominate. At later times such clusters display an $n(t)\sim t^\theta$ power law decay with $\theta\approx-0.4$, which agrees with the value expected for coarsening via patch coalescence in the nonhydrodynamical regime [24]. This scenario is confirmed visually, as well as by characteristic jumps in the (size weighted) average cluster size. Interestingly, we do not observe evidence for a Lifshitz-Slyozov type ripening, for which one would have $\theta=-2/3$ [25].

Having demonstrated the key features of the present model, including its tunability and its application to multicomponent systems, we now turn to performance aspects. Although one of the clear advantages of our approach is speed, it is difficult to make meaningful comparisons across different computer architectures and implementations. One basic quantity that provides a rough implementation-independent comparison is the particle number. Simulating a vesicle with 16 000 coarse grained lipids, as in our example, would require roughly 25 times as many solvent particles

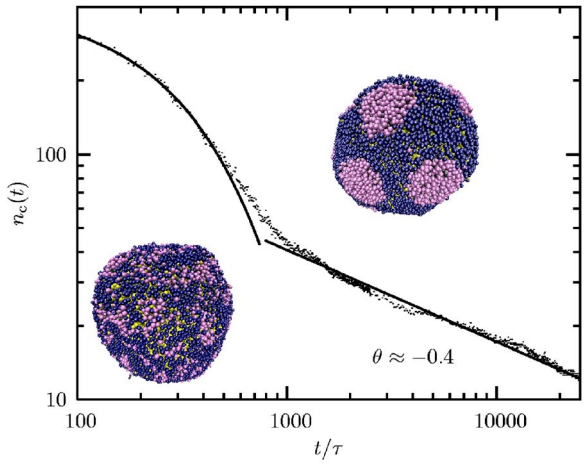

FIG. 4. (Color online) Coarsening kinetics for a vesicle composed of 4800 A lipids and 11200 B lipids at $k_BT=1.1\epsilon$ with self-interactions $w_c^{AA}=w_c^{BB}=1.7\sigma$. A cross term of $w_c^{AB}=1.5\sigma$ was imposed at $t=0\tau$. The number $n(t)$ of clusters of size $\geqslant 3$ was averaged over five independent runs. After an initial exponential decrease, a power law with exponent -0.4 is observed.

[19,20]. (Actually this factor scales with the vesicle radius.) Obviously, one must also account for the time step which is often chosen somewhat larger in DPD simulations. Still, this leads us to an at least fivefold speed-up for the present method over DPD, and a crude comparison based on direct CPU time usage agrees with this estimate [26].

In summary, we have presented a method that is fundamentally different from existing coarse grained lipid membrane simulations that use explicit solvent. Our method should be seen as complementary to these techniques since it presents a compelling speed advantage, especially for systems in three dimensions (vesicles, bicontinuous phases). It does not naturally include volume constraints or hydrodynamics. Indeed, the model is inspired by the great success of simple "bead-spring" models used to study polymer systems in the Rouse regime. We have presented Langevin dynamics simulations here, but the simplicity of the model and concept easily permit implementation of other integrators or even Monte Carlo. Volume constraints should be relatively simple and efficient to include via the concept of a "phantom solvent" [27]. The particle based nature of the model and its tunable interactions allow for great flexibility such that components with different predetermined stiffness and lipid shape present no difficulty, and topological changes occur naturally. Despite its astounding simplicity our approach allows one to capture all these essential aspects of lipid bilayer physics within a single unified framework.

Note added in proof. After submission of our manuscript, we learned about an alternative model independently developed by Brannigan *et al.* [28]. Its ability to self-assemble into a fluid phase also appears to rely on the existence of a long-ranged attraction.

We thank Oded Farago, Friederike Schmid, Hiroshi Noguchi, and Bernward Mann for valuable discussions.

[1] H. Lodish, A. Berk, S. L. Zipursky, P. Matsudaira, D. Baltimore, and J. Darnell, *Molecular Cell Biology* (Freeman & Company, New York, 2000).
[2] D. P. Tieleman, S. J. Marrink, and H. J. C. Berendsen, Biochim. Biophys. Acta **1331**, 235 (1997); S. E. Feller, Curr. Opin. Colloid Interface Sci. **5**, 217 (2000); L. Saiz, S. Bandyopadhyay, and M. L. Klein, Biosci Rep. **22**, 151 (2002).
[3] G. Gompper and D. M. Kroll, in *Statistical Mechanics of Membranes and Surfaces*, 2nd ed., edited by D. R. Nelson *et al.* (World Scientific, Singapore, 2004).
[4] J.-M. Drouffe, A. C. Maggs, and S. Leibler, Science **254**, 1353 (1991).
[5] H. Noguchi and M. Takasu, Phys. Rev. E **64**, 041913 (2001); J. Chem. Phys. **115**, 9547 (2001); Biophys. J. **83**, 299 (2002); Phys. Rev. E **65**, 051907 (2002).
[6] O. Farago, J. Chem. Phys. **119**, 596 (2003).
[7] G. Brannigan, and F. L. H. Brown, J. Chem. Phys. **120**, 1059 (2004); G. Brannigan, A. C. Tamboli, and F. L. H. Brown, *ibid.* **121**, 3259 (2004).
[8] http://www.espresso.mpg.de.
[9] G. S. Grest and K. Kremer, Phys. Rev. A **33**, R3628 (1986).
[10] A. Kolb and B. Dünweg, J. Chem. Phys. **111**, 4453 (1999).
[11] For brevity we have omitted a detailed analysis of the gel-liquid transition. These issues will be treated elsewhere.
[12] R. Kwok and E. Evans, Biophys. J. **35**, 637 (1981).
[13] D. Needham and R. S. Nunn, Biophys. J. **58**, 997 (1990).
[14] This is likely a finite-size effect [Brannigan, Tamboli, and Brown (Ref. [7]) observe a similar ensemble dependence].
[15] The LJ potential corresponds to $w_c \approx 0.7\sigma$ and has indeed historically proven to be unsuccessful in creating fluid bilayers.
[16] U. Seifert, Adv. Phys. **46**, 13 (1997).
[17] R. Lipowsky and S. Grotehans, Europhys. Lett. **23**, 599 (1993).
[18] R. Lipowsky, Biophys. J. **64**, 1133 (1993).
[19] S. Yamamoto and S. Hyodo, J. Chem. Phys. **118**, 7937 (2003).
[20] M. Laradji and P. B. Sunil Kumar, Phys. Rev. Lett. **93**, 198105 (2004).
[21] P. B. Sunil Kumar, G. Gompper, and R. Lipowsky, Phys. Rev. Lett. **86**, 3911 (2001).
[22] S. L. Veatch, and S. L. Keller, Phys. Rev. Lett. **89**, 268101 (2002); Biophys. J. **85**, 3074 (2003); T. Baumgart, S. T. Hess, and W. W. Webb, Nature (London) **425**, 821 (2003).
[23] T. Taniguchi, Phys. Rev. Lett. **76**, 4444 (1996).
[24] K. Binder and D. Stauffer, Phys. Rev. Lett. **33**, 1006 (1974).
[25] D. A. Huse, Phys. Rev. B **34**, 7845 (1986).
[26] Our 16 000 lipid vesicle takes $\sim$58 CPU h to complete 2000τ on a 2.0 GHz AMD Opteron246. This compares with $\sim$300 CPU h for a recent DPD simulation (Ref. [20]).
[27] O. Lenz and F. Schmid, J. Mol. Liq. **117**, 147 (2005).
[28] G. Brannigan, P. F. Phillips, and F. L. H. Brown, Phys. Rev. E **72**, 011915 (2005).